ACS Chemical Neuroscience

pubs.acs.org/chemneuro Research Article

Different Inhibitors of Aβ42-Induced Toxicity Have Distinct Metal-Ion Dependency

Ashley J. Mason,[#] Ian Hurst,[#] Ravinder Malik, Ibrar Siddique, Inna Solomonov, Irit Sagi, Frank-Gerrit Klärner, Thomas Schrader, and Gal Bitan*

Cite This: ACS Chem. Neurosci. 2020, 11, 2243−2255 Read Online

ACCESS | Metrics & More | Article Recommendations | Supporting Information

ABSTRACT: Oligomers of amyloid β-protein (Aβ) are thought to be the proximal toxic agents initiating the neuropathologic process in Alzheimer's disease (AD). Therefore, targeting the self-assembly and oligomerization of Aβ has been an important strategy for designing AD therapeutics. In parallel, research into the metallobiology of AD has shown that Zn^{2+} can strongly modulate the aggregation of Aβ in vitro and both promote and inhibit the neurotoxicity of Aβ, depending on the experimental conditions. Thus, successful inhibitors of Aβ self-assembly may have to inhibit the toxicity not only of Aβ oligomers themselves but also of Aβ-Zn^{2+} complexes. However, there has been relatively little research investigating the effects of Aβ self-assembly and toxicity inhibitors in the presence of Zn^{2+}. Our group has characterized previously a series of Aβ42 C-terminal fragments (CTFs), some of which have been shown to inhibit Aβ oligomerization and neurotoxicity. Here, we asked whether three CTFs shown to be potent inhibitors of Aβ42 toxicity maintained their activity in the presence of Zn^{2+}. Biophysical analysis showed that the CTFs had different effects on oligomer, β-sheet, and fibril formation by Aβ42-Zn^{2+} complexes. However, cell viability experiments in differentiated PC-12 cells incubated with Aβ42-Zn^{2+} complexes in the absence or presence of these CTFs showed that the CTFs completely lost their inhibitory activity in the presence of Zn^{2+} even when applied at 10-fold excess relative to Aβ42. In light of these results, we tested another inhibitor, the molecular tweezer CLR01, which coincidentally had been shown to have a high affinity for Zn^{2+}, suggesting that it could disrupt both Aβ42 oligomerization and Aβ42-Zn^{2+} complexation. Indeed, we found that CLR01 effectively inhibited the toxicity of Aβ42-Zn^{2+} complexes. Moreover, it did so at a lower concentration than needed for inhibiting the toxicity of Aβ42 alone. In agreement with these results, CLR01 inhibited β-sheet and fibril formation in Aβ42-Zn^{2+} complexes. Our data suggest that, for the development of efficient therapeutic agents, inhibitors of Aβ self-assembly and toxicity should be examined in the presence of relevant metal ions and that molecular tweezers may be particularly attractive candidates for therapy development.

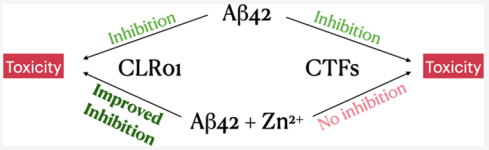

KEYWORDS: *Amyloid, Alzheimer's disease, metal ions, inhibitor, aggregation, neurotoxicity*

INTRODUCTION

Amyloid β-protein (Aβ) self-assembly into neurotoxic oligomers and aggregates is a seminal pathological process in Alzheimer's disease (AD).[1,2] Although deposition of fibrillar Aβ aggregates in amyloid plaques originally led to the *Amyloid Cascade Hypothesis*,[3,4] nonfibrillar Aβ oligomers are now considered by most researchers to be the true culprit causing the initial disruption of synaptic communication and instigating the cascade of events that leads to AD.[5−11] The other offending protein self-assembly process in AD, that of hyperphosphorylated tau, is believed to be secondary to the initial Aβ insults.[12] Therefore, targeting Aβ oligomers, particularly those of the longer and more toxic form, Aβ42, is a popular strategy for therapy development.[13]

In parallel, research into the metallobiology of AD has identified several metal ions that interact with Aβ, modulate its self-assembly and toxicity, and may be important for the onset and progression of the disease.[14,15] Metal cations, such as Zn^{2+}, Cu^{2+}, and Fe^{3+}, have been reported to stimulate the deposition of Aβ and promote the hyperphosphorylation of tau.[16,17] Much of the research has focused on the effects of Cu^{2+} and Zn^{2+} due to their role in the maintenance of neuronal excitability, their function as cofactors, and their contribution to oxidative stress and inflammation in the AD brain.[18] In addition, both ions have been shown to modulate the oligomerization and aggregation of Aβ itself.[19−22]

Zn^{2+} has been of particular interest due to its presence in deposited amyloid plaques and its concentration in glutamatergic neurons in the hippocampus.[23,24] Interestingly, Zn^{2+} ions have been reported to both accelerate and inhibit Aβ aggregation and both increase Aβ neurotoxicity and protect against Aβ neurotoxicity, depending on the specific conditions used by each group, including the concentration of Aβ and

Received: April 7, 2020
Accepted: June 19, 2020
Published: June 19, 2020

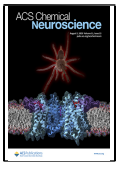

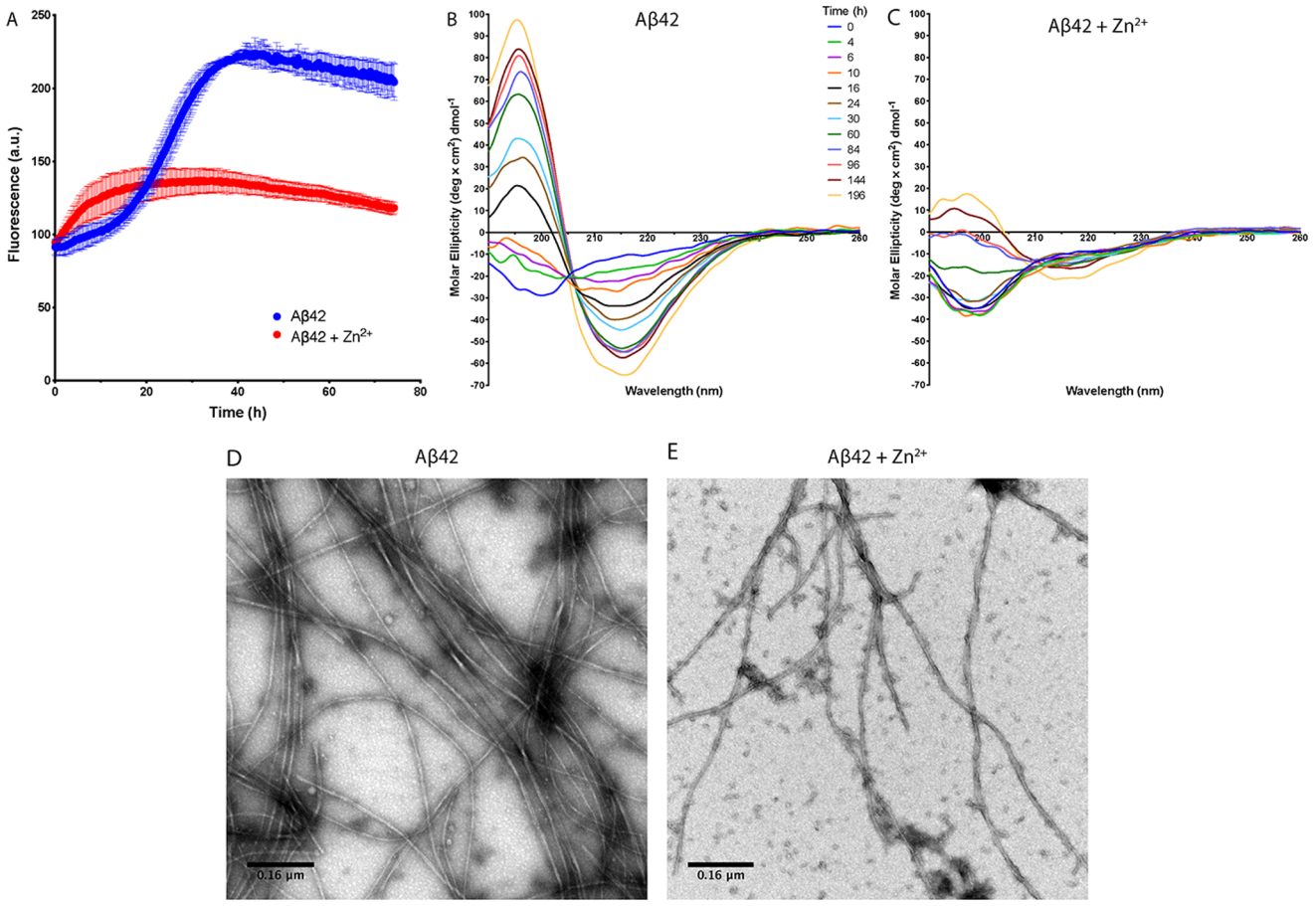

Figure 1. Aβ42 aggregates differently in the absence or presence of Zn^{2+}. Twenty micromolar Aβ42 was incubated in the absence or presence of 40 μM Zn^{2+}. (A) ThT fluorescence was measured every 15 min in five technical replicates per condition. (B, C) Representative CD spectra in aggregation reactions of Aβ42 (B) and Aβ42-Zn^{2+} (C). (D, E) Representative electron micrographs of Aβ42 (D) and Aβ42-Zn^{2+} (E) after 408 h of incubation. Scale bars represent 0.16 μM.

Zn^{2+}, the ratio between these concentrations, and the solution conditions.[24−29] Indeed, our own work showed that Zn^{2+} accelerated formation of nonfibrillar, yet β-sheet rich, aggregates of Aβ40 and that the toxicity of Aβ40-Zn^{2+} complexes depended on the method of their addition to cultured neurons.[30]

In the AD brain, high concentrations (~1 mM) of Zn^{2+} have been found in amyloid plaques along with elevated levels in the hippocampus and serum of patients.[31] Zn^{2+} concentrations up to 300 μM have been measured in synaptic vesicles[32,33] and during synaptic transmission, and direct imaging of Zn^{2+} using fluorescent probes has shown a release of 10−30 μM of Zn^{2+} into the synaptic cleft.[34] It is predominantly under these circumstances that free Zn^{2+} is thought to associate with Aβ[32,35−37] and induce the formation of neurotoxic assemblies.[32,38] Previously, we found that Aβ40-Zn^{2+} complexes were β-sheet-rich, nonfibrillar, quasi-spherical aggregates that suppressed spontaneous Ca^{2+} transients and were toxic to primary hippocampal neurons when added at small concentrations in several portions, but not when added at a higher concentration in the beginning of the experiment.[30] These findings led us to ask how the presence of Zn^{2+} might impact the interaction of Aβ assembly inhibitors/modulators with Aβ and whether such inhibitors maintained their inhibitory activity in the presence of Zn^{2+}.

Therapy development efforts targeting Aβ−metal-ion interactions have focused on chelators, such as clioquinol, a hydroxyquinoline-derived drug, which was shown to prevent cognitive decline in Zn^{2+}-transporter knockout mice,[39,40] and its successor, PBT2, which was found to lower Aβ levels in the CSF of patients with AD.[41] More recently, several compounds have been reported to have both metal-ion chelating activity and act as Aβ assembly inhibitors regardless of metal binding.[42−49] However, the latter activity may arise from the weak nature of the forces mediating Aβ oligomerization, which is easily modulated by many small molecules nonspecifically,[13] potentially through the formation of colloids.[50]

Previously, we reported that certain C-terminal fragments (CTFs) of Aβ42 interacted with the full-length peptide, modulated its oligomerization, and inhibited its toxicity.[51−54] In particular, out of 15 peptides with the general formula Aβ(x−42), where x = 28−39, Aβ(31−42) and Aβ(39−42) had notably high inhibitory activity. In addition, an Aβ40 CTF that originally was tested as a control, Aβ(30−40), was found to be a potent inhibitor of Aβ42-induced toxicity.[55] Thus, we decided to use these CTFs as a test case and determine how their inhibitory activity might be affected by the presence of Zn^{2+}. We studied the effect of the CTFs on the conformational change kinetics and morphology of Aβ42-Zn^{2+} complexes and on their toxicity in cell culture. We show that the CTFs' effects on Aβ42 β-sheet formation, morphology, and cytotoxicity are

https://dx.doi.org/10.1021/acschemneuro.0c00192
ACS Chem. Neurosci. 2020, 11, 2243−2255

dramatically altered by the interactions of Aβ42 with Zn^{2+}. In light of these results, we also tested another inhibitor of Aβ self-assembly and toxicity, the molecular tweezer CLR01, and found that its activity also was affected by the presence of Zn^{2+}, but in a distinct way.

RESULTS AND DISCUSSION

Zn^{2+} Alters Aβ42 Assembly and Toxicity. Because the CTFs were originally conceived as potential inhibitors of Aβ42, here we characterized first the aggregation and toxicity of Aβ42 in the presence of Zn^{2+}. In our previous study of Aβ40-Zn^{2+} complexes, the biophysical characterization of the system was done primarily in a 3-(*N*-morpholino)propanesulfonic acid (MOPS) buffer.[30] An interesting finding was that the addition of Zn^{2+} reduced the increase in thioflavin T (ThT) fluorescence even though circular dichroism (CD) spectroscopy showed that Aβ40-Zn^{2+} complexes were rich in β-sheet. Therefore, we used both techniques here again to assess the temporal conformational changes in Aβ42 in the presence of Zn^{2+}. However, initial attempts to characterize the temporal changes of Aβ42-Zn^{2+} complexes in MOPS buffer using CD spectroscopy yielded low signal-to-noise ratio spectra, because MOPS strongly absorbs light below 200 nm.[56] For this reason, we decided to change the buffer from MOPS to phosphate buffer (PB). Using PB, we found that reproducibility was low and data interpretation was difficult when using a concentration of Aβ42 below 20 μM. Therefore, although lower concentrations were used in our toxicity assays, the investigation of Aβ42 aggregation and conformational change in the presence of Zn^{2+} and the effect of the CTFs on this process was done using 20 μM Aβ42. To be able to compare these experiments with the toxicity assays, the Aβ42/Zn^{2+} concentration ratio was kept at 1:2, respectively, in all experiments.

In the absence of Zn^{2+}, Aβ42 showed a two-phased sigmoidal curve, consisting of a short lag phase of ∼3 h, a relatively slow increase up to ∼14 h, and a faster increase reaching a plateau at ∼42 h (Figure 1A). This rate of ThT fluorescence increase was slow relative to other reports in the literature, including from our own group, even when using lower concentrations of Aβ42.[24,27,57,58] In our experience, many factors influence the rate of the increase, including the peptide source and the exact preparation method, including the steps used for disaggregation and solubilization, peptide concentration, buffer type and concentration, salt type and concentration, pH, temperature, agitation method, and agitation rate. As explained above, we chose the conditions for these experiments to allow meaningful comparisons with the conditions in which Zn^{2+} and/or CTFs were added to the reaction mixture, taking into account that precise quantitative comparison with the multiple previous reports in the literature may not be possible due to the different conditions used in each study.

In contrast to Aβ42 alone, in the presence of 2 equiv of Zn^{2+}, no lag phase was observed. Rather, the ThT fluorescence increased rapidly during the first 8 h and reached a maximum at ∼16 h. However, the maximum fluorescence was substantially lower than the value for Aβ42 alone (Figure 1A), in agreement with the behavior of Aβ40 in the presence of Zn^{2+} reported previously.[30]

CD spectroscopy analysis of the Aβ42 conformation in the absence of Zn^{2+} showed a gradual transition from a predominantly statistical coil spectrum at t = 0, characterized by a minimum at 198−200 nm, to a primarily β-sheet spectrum at 196 h, displaying the typical maximum at 195−196 nm and minimum at 215−218 nm (Figure 1B). In the presence of Zn^{2+}, an overall transition from statistical coil to β-sheet also was observed (Figure 1C), but with two important differences. First, unlike the gradual conformation change observed in the spectra of Aβ42 alone already at early time points, in the presence of Zn^{2+} the spectra remained largely unchanged for the first 24 h, suggesting a delay in the conformational transition. Second, the amplitude of the spectra in the presence of Zn^{2+} was substantially reduced compared to the spectra of Aβ42 alone, suggesting overall smaller changes in the presence of Zn^{2+}. These data suggested that, upon addition of Zn^{2+} to Aβ42, Aβ42-Zn^{2+} complexes formed rapidly, and although they changed over time, the change involved relatively minor conformational rearrangements.

Interestingly, the rapid increase in ThT fluorescence (Figure 1A) disagreed with the small change in conformation observed by CD during this time (Figure 1B), suggesting that, in the presence of Zn^{2+}, ThT might bind rapidly to Aβ42-Zn^{2+} complexes without formation of substantial β-sheet conformation. The binding may involve a ternary complex formed by the protein, the metal ion, and the dye molecules, yet it is an atypical phenomenon that does not actually report on the formation of a cross-β structure or of amyloid fibrils, as would be expected in a typical ThT-fluorescence experiment. In agreement with this interpretation, the overall magnitude of the change in fluorescence during the reaction was only ∼30% compared to Aβ42 alone. An alternative explanation might stem from formation of insoluble aggregates that bind ThT but have little impact on the CD spectrum. We did not observe particulate matter in the solutions in either experiment, but we cannot rule out the formation of insoluble, ThT-positive aggregates that were too small to detect by the naked eye.

Morphological examination of each preparation by transmission electron microscopy (TEM) at intermediate time points (Supporting Information Figure S1) and at the end of the aggregation reaction (Figure 1D,E) showed that, during the reaction, oligomers and fibrils were observed, whereas at the end of the aggregation reaction, abundant fibrils were present in both cases. However, the abundance was higher in samples containing Aβ42 alone, in which some fibrils appeared thicker and comprised multiple thin filaments. Quasi-globular structures, presumably oligomers, also were observed but were relatively sparse in samples of Aβ42 alone. In the samples containing Aβ42-Zn^{2+} complexes, the fibrils were thinner on average than in those containing Aβ42 alone, and twisted fibrils appeared to comprise mainly two intertwined threads. The abundance of quasi-globular structures and amorphous aggregates in these samples was substantially higher than in samples of Aβ42 alone (Supporting Information Figure S1 and Figure 1D,E).

To measure the toxicity of Aβ42 in the absence or presence of Zn^{2+}, we employed a strategy developed in our previous study of Aβ40-Zn^{2+} complexes.[30] In that study, we found that, if 10 μM Aβ40-Zn^{2+} complexes were added to primary rat hippocampal neurons all at once, they did not cause measurable toxicity 48 h later, likely because under these conditions the formation of toxic structures was transient and too short before the complexes transformed into larger, nontoxic aggregates.[30] In contrast, if the sample was divided into four equal portions, each of which was prepared freshly and added 12 h apart, more than 80% of the cells were found

https://dx.doi.org/10.1021/acschemneuro.0c00192
ACS Chem. Neurosci. 2020, 11, 2243−2255

to be dead at 48 h using a neuron-specific enolase assay. Here, we used differentiated PC-12 cells and the lactate dehydrogenase (LDH) assay to measure cell viability. First, we confirmed that upon addition of Aβ42-Zn^{2+} complexes in one portion to the cells, little toxicity was observed after a 48 h incubation (3.8 ± 2.0% cell death, Figure 2) compared to Aβ42 alone

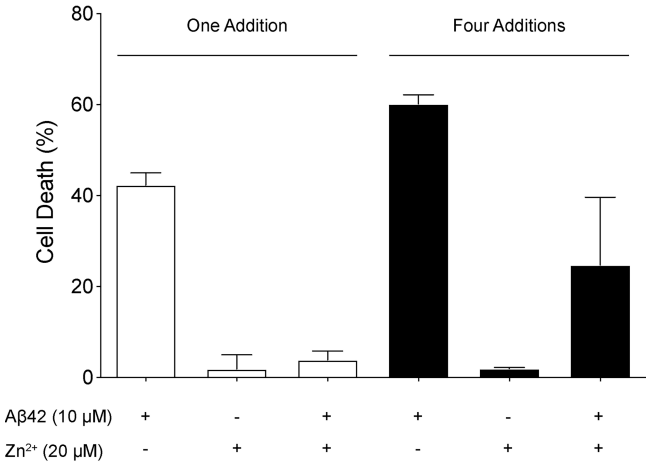

Figure 2. Aβ42-Zn^{2+}complexes are toxic when added in small portions. Aβ42 was prepared in the absence or presence of Zn^{2+}, and the same total amount was added to differentiated PC-12 cells either at time 0 or in four equal portions at times 0, 12, 24, and 36 h. Cell death was measured using the LDH assay at 48 h. Each column is an average of three or four biological replicates, each done in six technical replicates. The error bars represent the standard error of measure (SEM).

(42.3 ± 2.7% cell death). Zn^{2+} on its own was not toxic under these conditions (1.9 ± 3.1% cell death). Therefore, we adopted the previously established protocol,[30] added a fresh aliquot equal to a quarter of each sample at t = 0, 12, 24, and 36 h, and measured cell viability at 48 h. Under these conditions Aβ42 showed increased toxicity (60.1 ± 2.0% cell death), Zn^{2+} was not toxic (1.9 ± 0.3% cell death), and Aβ42-Zn^{2+} complexes gave somewhat variable results, but overall were ∼6 times more toxic than when added in one portion (24.7 ± 14.9% cell death, Figure 2). Therefore, we used the four-portion paradigm in all the toxicity-inhibition experiments.

CTFs Have Distinct Effects on the Self-Assembly of Aβ42-Zn^{2+} Complexes. To test the effect of Aβ(39−42), Aβ(31−42), and Aβ(30−40) on the aggregation of Aβ42-Zn^{2+} complexes, we incubated mixtures of 20 μM Aβ42, 40 μM Zn^{2+}, and 100 μM of each CTF at 37 °C with agitation and measured the change in ThT fluorescence and CD spectra during the aggregation reactions. In control ThT experiments, the CTFs were examined on their own or in the presence of Zn^{2+} at the same concentrations. Compared to Aβ42-Zn^{2+} alone (Figure 3A), the ThT signal of Aβ42-Zn^{2+} in the presence of Aβ(39−42) increased initially at a similar rate, whereas the final fluorescence was ∼25% lower (Figure 3A, blue curve). In contrast, a markedly different behavior was observed in the presence of Aβ(31−42) or Aβ(30−40). In both cases, the initial fluorescence was ∼5 times higher than in the presence of Aβ42-Zn^{2+} alone or Aβ42-Zn^{2+} in the presence of Aβ(39−42), suggesting a rapid formation of quaternary complexes comprising Aβ42, Zn^{2+}, the CTF, and ThT. This interpretation was supported by the observation that Zn^{2+} had a minimal impact on the behavior of the CTFs on their own (Figure 3B). Aβ(39−42) and Aβ(31−42) showed essentially no change in fluorescence during the experiment, regardless of the presence of Zn^{2+}. In contrast, the fluorescence of Aβ(30−40) showed a two-step increase followed by a slow decrease after 24 h. In the presence of Zn^{2+} the initial increase in ThT fluorescence was accelerated and was followed by a decrease up to ∼10 h and then a plateau (Figure 3B).

In the mixtures with Aβ42, Aβ(31−42) caused a rapid increase in the ThT fluorescence signal, which peaked at ∼18 h and then declined steadily until the end of the experiment

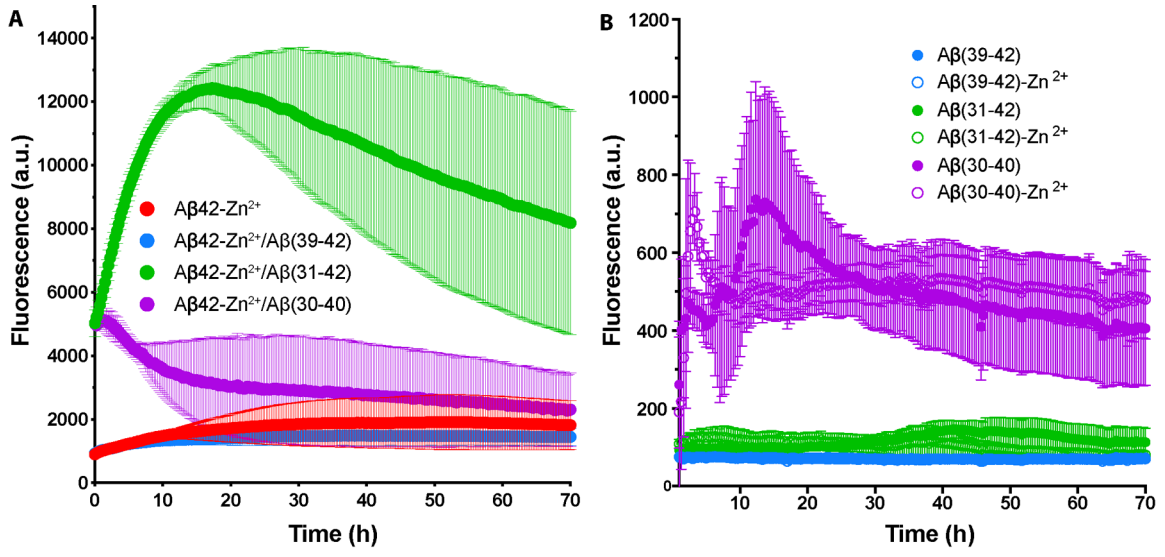

Figure 3. Time-dependent ThT fluorescence of Aβ42-Zn^{2+}complexes in the presence of CTFs. (A) Aβ42 (20 μM) and 40 μM Zn^{2+} were incubated in the absence or presence of 100 μM of each CTF, and the change in ThT fluorescence was monitored every 15 min and averaged for five technical replicates per condition. (B) The CTFs in the absence of Aβ42 were monitored at the same concentrations under the same conditions (though using a different plate reader, reflected by the different scales of the arbitrary fluorescence units on the y-axis of the two panels). Error bars represent the standard deviation (SD).

https://dx.doi.org/10.1021/acschemneuro.0c00192
ACS Chem. Neurosci. 2020, 11, 2243−2255

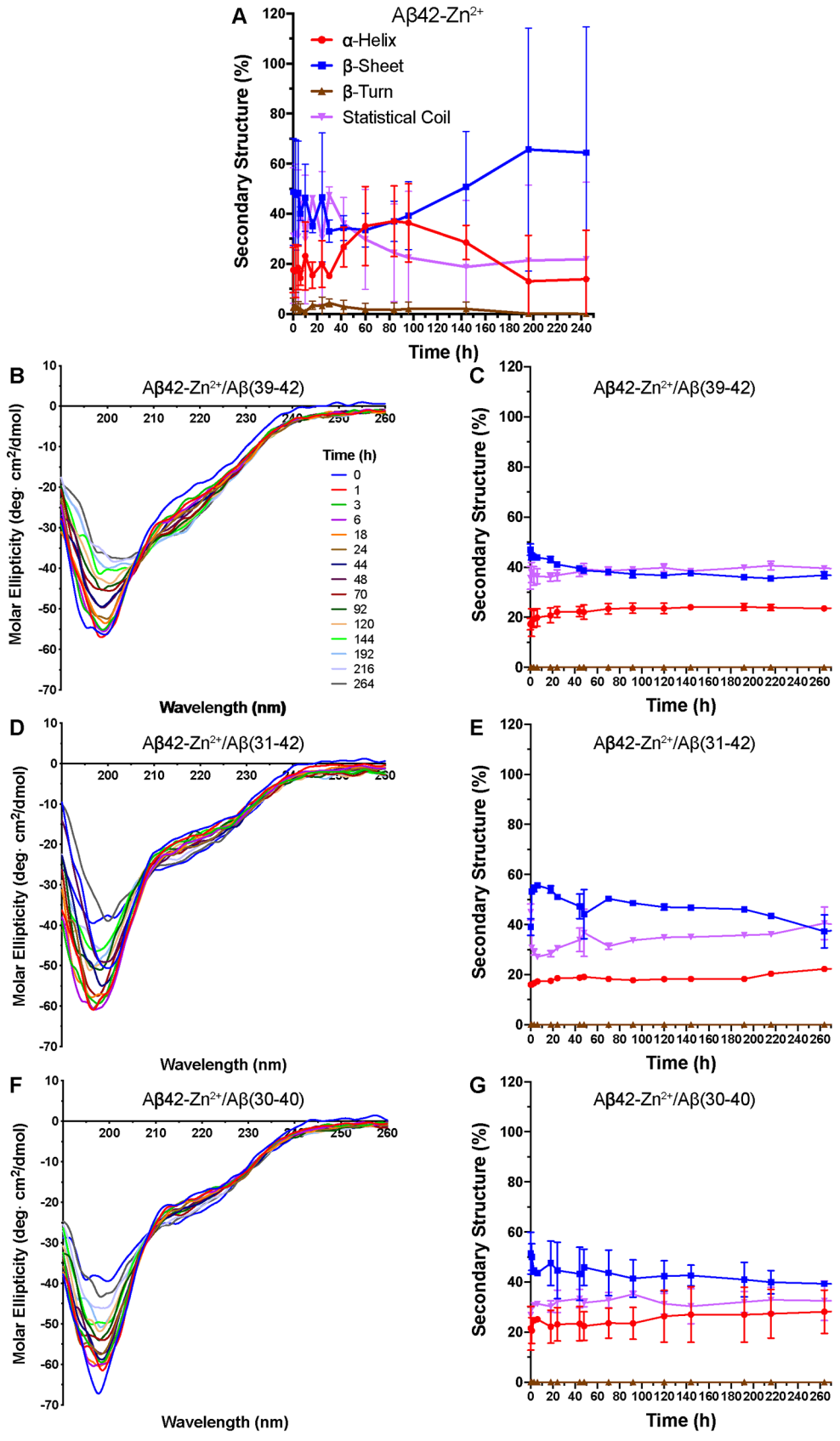

Figure 4. CD-spectroscopy analysis of Aβ42-Zn^{2+} complexes in the presence of CTFs. Twenty micromolar Aβ42 and 40 μM Zn^{2+} were incubated in the absence or presence of 100 μM of each CTF, and the change in CD spectrum was monitored at the times indicated in (B), which apply also to (D, F). (A) Deconvolution of the CD spectra shown in Figure 1C. (C, E, G) Deconvolution of the spectra shown in (B, D, F), respectively.

https://dx.doi.org/10.1021/acschemneuro.0c00192
ACS Chem. Neurosci. 2020, 11, 2243−2255

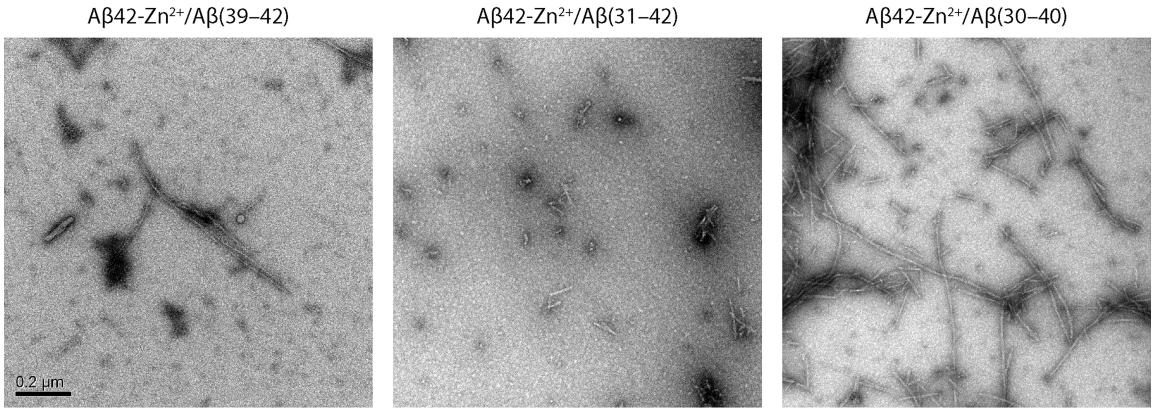

Figure 5. Morphological analysis of Aβ42-Zn^{2+} complexes in the presence of CTFs. Twenty micromolar Aβ42 and 40 μM Zn^{2+} were incubated in the absence or presence of 100 μM of each CTF. The morphology of the mixture was assessed using EM after 17 d of incubation. Representative electron micrographs are shown. The scale bar in the left image represents 0.2 μm and is applicable to all the images.

(Figure 3A). In the presence of Aβ(30−40) (Figure 3A), the fluorescence increased slightly in the first 90 min, then declined rapidly for the next ∼16 h, followed by a slower decline until the end of the experiment, at which point, the fluorescence was only a little higher than that of Aβ42-Zn^{2+} alone. Comparison of Figures 3A and B suggested that this behavior might have been influenced by the CTF itself and might not have reflected formation of a complex involving Aβ42 and Aβ(30−40), though formation of a complex could not be ruled out (the experiments in Figures 3A and B were done using different plate readers, and therefore the comparison is qualitative rather than quantitative). Interestingly, in the presence of Aβ42, in both the cases of Aβ(31−42) and Aβ(30−40), the behavior of the different replicates was highly consistent for the first 8 h of the experiment but then diverged substantially (Figure 3A). Nonetheless, despite the relatively low reproducibility among replicates between 8 and 72 h, the distinction among the behavior of the different mixtures was clear. These peculiar behaviors supported the idea that in these experiments ThT fluorescence either reflected formation of complexes that were different from the typical binding of the dye molecules to cross-β structures of amyloid fibrils or, in the case of Aβ(30−40), the ThT-fluorescence curve was dominated by the behavior of the CTF itself.

To further assess the change in secondary structure of Aβ42-Zn^{2+} complexes in the presence of CTFs, we examined the temporal changes in CD spectra of the same mixtures (prepared together but incubated without ThT) and deconvoluted the spectra to gain additional insight. CD spectra of the CTFs themselves have been reported previously[53] and therefore were not recorded here. Supporting the interpretation that the ThT data reflected atypical complexes rather than cross-β structures, unlike their distinct behavior in the ThT-fluorescence experiments, all three CTFs showed roughly similar attenuation of the conformational change in CD spectroscopy (Figure 4B,D,F). In all cases, the initial spectra were characteristic of a statistical coil. Over 11 d of incubation, relatively small changes were observed in the presence of the CTFs. The magnitude of the minimum at 195−198 nm decreased, and the molar ellipticity at the typical ∼215 nm minimum characteristic of a β-sheet slightly increased, yet those changes were relatively minor, and the final spectra suggested that the peptides (Aβ42 and CTF) were still largely unstructured in these complexes. Again, dissimilarity between the ThT and CD data might reflect the formation of ThT-positive insoluble aggregates that did not contribute to the CD spectra and were too small to detect by the naked eye.

To quantify the change, we deconvoluted the spectra using the Savitzky-Golay algorithm. In the absence of CTFs, Aβ42-Zn^{2+} complexes showed a somewhat variable behavior (Figure 4A; the data are an average of three experiments, including the one presented in Figure 1C). The conformational transition involved a temporary formation of an α-helical intermediate between 30 and 90 h, which decreased at later time points, concomitant with an increase in β-sheet content and a decline in statistical coil, as described previously for Aβ in the absence of Zn^{2+}.[59] In the presence of the CTFs, the variability between experiments was substantially lower, and the deconvolution showed only minor conformational changes during the reactions. In the presence of Aβ(39−42), which itself is expected to be unstructured,[53] the mixture comprised ∼40% each statistical coil and β-sheet, and ∼20% α-helix, with minimal changes in these fractions for the duration of the experiment (Figure 4C). In the presence of Aβ(31−42), similar initial fractions were observed at t = 0 h. In the next 3 h, the abundance of β-sheet conformation increased to ∼55%, and that of statistical coil decreased to ∼35%, possibly reflecting formation of β-sheet in the CTF itself.[53] Then, this trend was slowly reversed during the next 261 h, until the β-sheet and statistical coil fractions were again ∼40% each. The α-helix fraction remained at ∼20% throughout the entire reaction (Figure 4E). Aβ(30−40) caused formation of ∼50% β-sheet immediately at t = 0 h, followed by a slow decrease to ∼40% at 264 h, which was accompanied by minor increases in statistical coil, from 27% to 32%, and α-helix, from 21% to 28% (Figure 4G). Although the numbers generated by the deconvolution algorithm may not be precise, they provide an approximation of the contribution of each secondary structure component, supporting the conclusion that to a large extent the CTFs attenuated the conformational transition observed in Aβ42-Zn^{2+} complexes (Figures 1C and 4A).

Morphological analysis of the Aβ42-Zn^{2+} mixtures in the presence of each CTF at the end of the aggregation reaction showed mixtures of fibrillar and nonfibrillar structures (Figure 5). In all cases, the fibrils were shorter and less abundant than in mixtures of Aβ42-Zn^{2+} complexes formed in the absence of

https://dx.doi.org/10.1021/acschemneuro.0c00192
ACS Chem. Neurosci. 2020, 11, 2243−2255

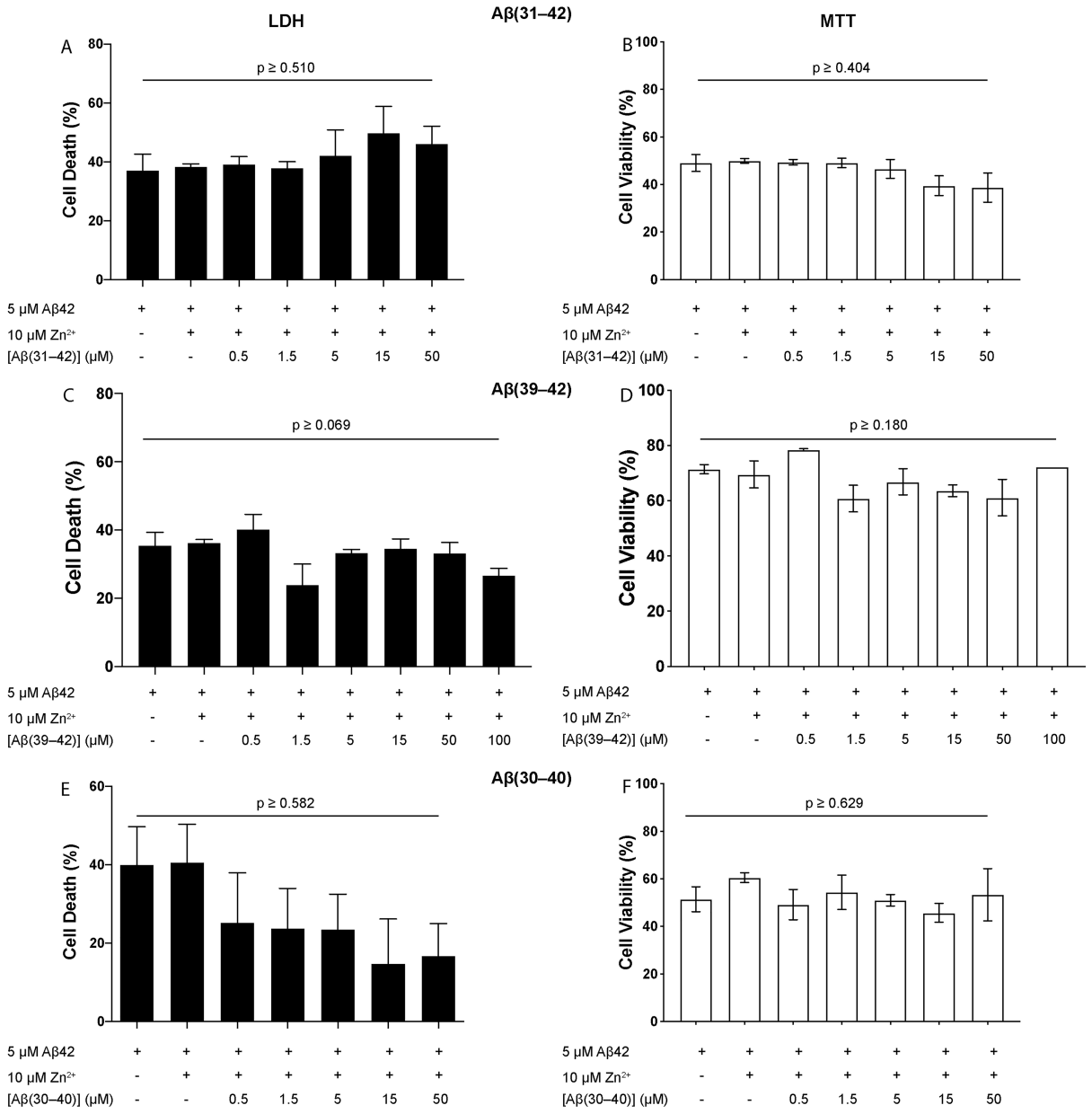

Figure 6. Evaluation of the cytotoxicity of Aβ42-Zn^{2+}complexes in the presence of CTFs. Five micromolar Aβ42 and 10 μM Zn^{2+} were prepared in the absence or presence of increasing concentrations of each CTF and added to differentiated PC-12 cells in four equal portions at times 0, 12, 24, and 36 h. (A, C, E) Cell death was measured at 48 h using the LDH-release assay. (B, D, F) Cell viability was measured at 48 h using the MTT-reduction assay. The data represent three biological replicates, each done with six technical replicates. Error bars indicate SEM. The *p*-values were calculated by a one-way ANOVA with a post hoc Tukey test for multiple comparisons. The value indicated in each panel is for the smallest *p*-value comparing any two columns.

CTFs. The shortest and thinnest fibrils appeared to form in the presence of Aβ(31−42) (Figure 5B), whereas the longest and most abundant fibrils formed in the presence of Aβ(30−40) (Figure 5C). These fibrils were still shorter than those formed by Aβ42 in the presence of Zn^{2+} in the absence of CTFs (Figure 1E), whereas in the presence of Aβ(39−42) an intermediate effect was observed. These results suggest that the C-terminal residues of Aβ42, namely, Ile^{41}-Ala^{42}, which are missing in Aβ(30−40), contribute to the interference of the CTFs with fibril formation. The relatively low abundance of the fibrils agreed, in general, with the CD spectroscopy data, though the differences in morphology among the mixtures containing different CTFs were more pronounced than the differences in conformational transition as reflected by the CD spectra.

CTFs Do Not Inhibit the Toxicity of Aβ42-Zn^{2+} Complexes. We then used the LDH-release and 3-(4,5-dimethylthiazol-2-yl)-2,5-diphenyltetrazolium bromide (MTT)-reduction assays to assess if the addition of Zn^{2+} to Aβ42 would impact the inhibitory activity of CTFs. In our previous work, Aβ(31−42) and Aβ(39−42) were shown to inhibit the toxicity of 5 μM Aβ42 with half-maximal inhibition (IC_{50}) values of 20 ± 4 and 47 ± 14 in the LDH-release assay,[51] whereas Aβ(30−40) yielded IC_{50} = 29 ± 4 μM in the LDH assay under similar conditions.[54] Remarkably, in the presence of Zn^{2+} (i.e., complexes comprising 5 μM Aβ42 and 10 μM Zn^{2+}), all three CTFs lost completely their inhibitory

https://dx.doi.org/10.1021/acschemneuro.0c00192
ACS Chem. Neurosci. 2020, 11, 2243−2255

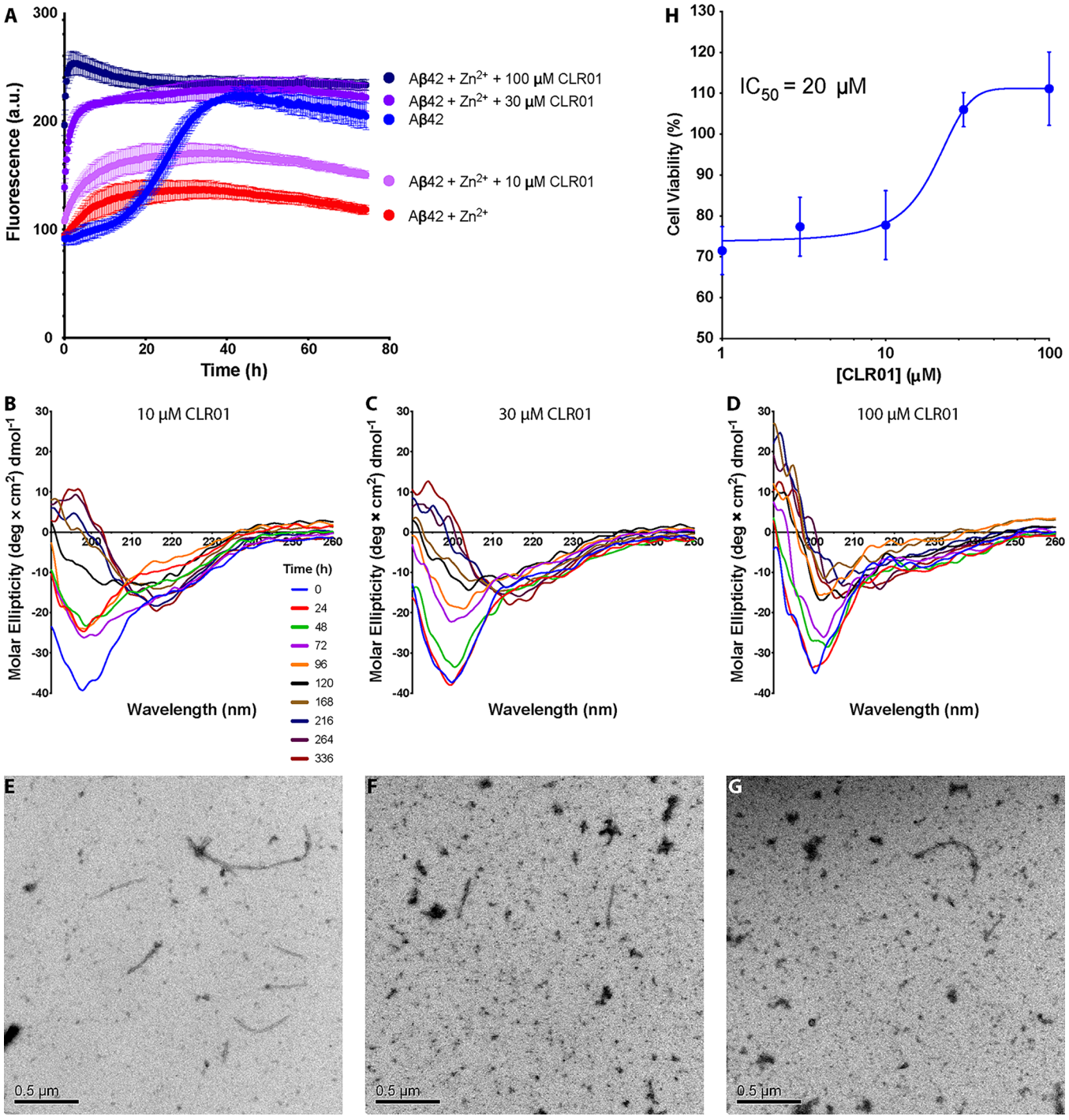

Figure 7. Effect of CLR01 on secondary structure, morphology, and toxicity of Aβ42-Zn^{2+} complexes. (A) Twenty micromolar Aβ42 and 40 μM Zn^{2+} were incubated in the absence or presence of 10, 30, or 100 μM of CLR01, and the change in ThT fluorescence was monitored every 15 min and averaged for five technical replicates per condition. Error bars represent SD. (B–D) CD spectra of aggregation reactions, similar to those in (A) and monitored at the times indicated in (B), which apply also to (C, D). (E–G) Electron micrographs of the same reaction mixtures used for the corresponding CD experiments at the end of the reaction. (H) Five micromolar Aβ42 and 10 μM Zn^{2+} were dissolved in the absence or presence of increasing concentrations of CLR01 and added to differentiated PC-12 cells in four equal portions at times 0, 12, 24, and 36 h. Cell viability was measured at 48 h using the MTT assay. Each data point represents three or four biological replicates, each done with six technical replicates. IC_{50} was calculated using Prism 8.4.0 by nonlinear fitting with four-parameter variable slope. The program did not allow calculating the error of the IC_{50} value due to the magnitude of the experimental error.

activity even when used at 10-fold excess (20-fold excess in the case of Aβ(39–42), Figure 6), suggesting that the structures of the Aβ42-Zn^{2+} complexes and/or their interaction with the cells were distinct from those of Aβ42 oligomers formed in the absence of Zn^{2+}.

CLR01 Modulates Aβ42 Assembly and Inhibits Its Toxicity in the Presence of Zn^{2+}. In light of these results, we asked whether other inhibitors acting by different mechanisms could still inhibit the formation or toxicity of the Aβ42-Zn^{2+} complexes and tested whether a similar loss of

https://dx.doi.org/10.1021/acschemneuro.0c00192
ACS Chem. Neurosci. 2020, 11, 2243–2255

inhibition would be observed for the molecular tweezer CLR01. CLR01 is a broad-spectrum inhibitor,[60−62] which previously has been shown to prevent the conformational change of Aβ42 in ThT-fluorescence and CD-spectroscopy assays and inhibit the toxicity of Aβ42 in differentiated PC-12 cells with IC_{50} = 52 ± 18 μM in the MTT-reduction assay.[57] CLR01 is a particularly interesting test case for inhibiting the toxicity of Aβ42-Zn^{2+} complexes, because it could target both Aβ42 and Zn^{2+} simultaneously. Its binding to Zn^{2+} was reported by Wilch et al., who discovered that CLR01 bound Zn^{2+} with a relatively high affinity, K_d = 5 μM, as opposed to a number of other metal ions, including Fe^{3+}, Cu^{2+}, Cs^{+}, Ca^{2+}, and Mg^{2+}, for which CLR01 had low or no affinity.[63] Interestingly, binding of CLR01 to Zn^{2+} appeared to be cooperative, rather than competitive, with binding to Lys. ^{1}H NMR spectroscopy and fluorescence titrations suggested that CLR01 chelated Zn^{2+} by both phosphate groups while maintaining binding to a Lys side-chain inside its cavity.[63] However, how simultaneous binding to Lys and Zn^{2+} affects the affinity of CLR01 for either ligand is not known.

The impact of 10, 30, or 100 μM CLR01 on temporal changes of ThT fluorescence in a solution of complexes made of 20 μM Aβ42 and 40 μM Zn^{2+} showed a rapid increase in ThT fluorescence without a lag phase, similar to Aβ42-Zn^{2+} in the absence of CLR01 (Figure 7A). The slope and final fluorescence value increased dose-dependently with CLR01 concentration. This behavior was distinct from the effect of CLR01 on the behavior of Aβ42 in the ThT-fluorescence assay in the absence of Zn^{2+}, which was a typical inhibition, that is, a longer lag time, slower increase, and reduced final fluorescence at a 1:1 concentration ratio and near quantitative inhibition (no increase in fluorescence) at 3- or 10-fold excess CLR01.[57] However, the rapid increase in ThT fluorescence without a lag phase, observed here upon addition of CLR01 to Aβ42 in the presence of Zn^{2+}, was similar to the effect of CLR01 on ThT fluorescence in the presence of other amyloidogenic proteins for which the rapid increase in fluorescence correlated with formation of nonfibrillar structures,[57,64] suggesting that, in this case as well, the fluorescence increase reported on formation of nonamyloid complexes. In support of this interpretation, CD spectroscopy showed that the conformational transition in the presence of low concentrations of CLR01, 10 or 30 μM (Figures 7B, C, respectively), resembled that of Aβ42-Zn^{2+} complexes (Figure 1C) rather than that of Aβ42 alone (Figure 1B). In the presence of 100 μM CLR01, although a gradual change in the CD spectrum suggested a slow conformational change, the spectra were consistent with a statistical coil at all times and showed no formation of β-sheet. Thus, we conclude that, despite the sharp and rapid increase in ThT fluorescence in mixtures containing Aβ42, Zn^{2+}, and CLR01, the fluorescence does not reflect formation of a cross-β structure. In agreement with this interpretation, the morphologies observed in the samples at the end of 14 d of incubation consisted of a mixture of short, thin fibrils and oligomer-like structures when CLR01 was present at a substoichiometric concentration (Figure 7E), whereas mostly oligomers and very rare fibrillar structures were observed in the presence of 30 or 100 μM CLR01 (Figures 7F and G, respectively.

Evaluation of the toxicity of Aβ42-Zn^{2+} complexes in the presence of increasing CLR01 concentrations using the MTT reduction assay showed that, unlike the CTFs, CLR01 effectively inhibited the toxicity of Aβ42 in the presence of Zn^{2+}. Dose−Response analysis showed that the IC_{50} of CLR01 in this assay was 20 μM (Figure 7H). This value was ∼2.5 times lower than the IC_{50} for CLR01 inhibition of Aβ42 in the absence of Zn^{2+}, suggesting not only that CLR01 is a better inhibitor of the toxicity of Aβ42-Zn^{2+} complexes than the CTFs but also that its ability to bind Zn^{2+} may act cooperatively with binding to Lys for inhibition of Aβ42-induced toxicity.

Our study of peptides derived from the C-terminus of Aβ42 and the molecular tweezer CLR01 show that, although the two types of compounds inhibit the toxicity of Aβ42 on its own in cell culture with half-maximal inhibition in the micromolar range, the CTFs completely lose their ability to inhibit the toxicity in the presence of Zn^{2+}, whereas CLR01 not only remains an effective inhibitor but even gains inhibitory activity.

Biophysical investigation established that, under the conditions we used, the presence of Zn^{2+} altered the self-assembly of Aβ42 into formation of a mixture of fibrils and oligomers (Figure 1E), in which the β-sheet content was lower (Figure 1C) than in fibrils of Aβ42 in the absence of Zn^{2+} (Figure 1B). As we reported previously for Aβ40,[30] Zn^{2+} altered dramatically the interaction of ThT with Aβ42. A rapid, relatively small increase in the fluorescence, without a lag phase, was observed in mixtures of Aβ42 and Zn^{2+}, but it apparently reflected the formation of atypical ternary complexes in which presumably the ThT molecules were rather flat, leading to the observed increase in their fluorescence. This was evidenced by the absence of substantial β-sheet structure in the CD spectra at the corresponding time points. Similar to Aβ40-Zn^{2+} complexes, the Aβ42-Zn^{2+} complexes did not show toxicity when applied to cultured cells all at once, presumably due to rapid aggregation into benign structures.[30] However, when the same total amount of Aβ42-Zn^{2+} complexes was added in four portions over 36 h, their toxicity was substantially higher, likely because, under these conditions, the concentration of the complexes did not allow formation of large, nontoxic aggregates.

The behavior of the ThT fluorescence of Aβ42-Zn^{2+} complexes in the presence of the inhibitor compounds further supports the conclusion that this fluorescence did not reflect formation of β-sheet-rich fibrils. The only inhibitor that slightly reduced the fluorescence was Aβ(39−42) (Figure 3A), which previously had been shown not to affect the ThT increase upon fibrillation of Aβ42 in the absence of Zn^{2+}.[58] In contrast, Aβ(30−40), Aβ(31−42), and CLR01 all caused an immediate increase in the ThT fluorescence (Figures 3A and 7A) followed by gradual changes that did not correlate with the degree of β-sheet formation evidenced by CD spectroscopy (Figures 4 and 7B−D). We conclude that ThT fluorescence is not a reliable method for measurement of β-sheet formation or amyloid fibrils by Aβ42 (or Aβ40[30]) in the presence of Zn^{2+}.

In contrast to the ThT fluorescence, the CD spectra did not seem to suffer from artifacts and reported on changes in the secondary structure of the Aβ42-Zn^{2+} complexes in a manner that appeared consistent with the morphological evaluation and toxicity measurement. As deconvolution algorithms rely on sampling of known structures and can lead to overfitting of the data, we focus the discussion on the spectral changes themselves. In the presence of fivefold excess of the CTFs (Figure 4B−G) or CLR01 (Figure 7B−D), little conformational change was observed over multiple days of incubation, suggesting that the peptides remained predominantly unstructured. Previously, little to no change was observed in solutions of Aβ(39−42) or Aβ(30−40) incubated on their own at ∼200

https://dx.doi.org/10.1021/acschemneuro.0c00192
ACS Chem. Neurosci. 2020, 11, 2243−2255

μM, suggesting that these peptides did not form β-sheets, whereas Aβ(31−42) incubated at ∼60 μM gradually formed β-sheet-rich fibrils over 48 h.[53] Here, despite being used at a higher concentration, 100 μM, little conformational change was observed over time for all the CTFs, supporting the interpretation that they formed relatively stable ternary complexes with Aβ42 and Zn^{2+}. The larger amplitude of the spectra in the presence of the CTFs, where the value of the minimum at 195 nm was 60−70 deg × cm^2 $dmol^{-1}$, in comparison to those in the presence of CLR01, where the minimum was ∼40 deg × cm^2 $dmol^{-1}$, likely reflects the contribution of the CTFs themselves. This behavior suggested that all the inhibitors reduced the tendency of the Aβ42-Zn^{2+} complexes to form fibrils. Indeed, morphological analysis showed shorter, thinner, and less-abundant fibrils in the presence of the CTFs (Figure 3) than in their absence (Figure 1E). This effect was stronger in the presence of Aβ(31−42) and Aβ(39−42) than in the presence of Aβ(30−40), suggesting that the Ile^{41}-Ala^{42} dipeptide contributed to the disruption of Aβ42-Zn^{2+} fibril formation. Inhibition of fibril formation by CLR01 was stronger than by the CTFs, even at low concentrations (cf. Figure 5 and Figure 7E−G). In the presence of all the inhibitors, the suppression of fibril formation appeared to increase the presence of oligomer-like structures.

In previous studies of the CTFs and CLR01 as inhibitors of Aβ42 self-assembly and toxicity, we proposed that all the inhibitors stabilized oligomeric structures (we termed them hetero-oligomers in the case of the CTFs[51]), which unlike the oligomers formed by Aβ42 itself, were nontoxic in multiple cell-culture systems.[51,52,54,55,57,65,66] Here, we discovered that although both the CTFs and CLR01 appeared to suppress fibrillogenesis of Aβ42-Zn^{2+} complexes, thereby increasing the relative abundance of nonfibrillar oligomers, the oligomers formed in the presence of the three CTFs maintained their toxicity (Figure 6), whereas those formed in the presence of CLR01 were nontoxic at concentrations of at least 30 μM (Figure 7H). This opposite effect of the addition of Zn^{2+} on the ability of the two types of inhibitors to suppress Aβ42 toxicity is remarkable and suggests that Aβ inhibitors evaluated in cell culture should be tested not only against the peptide itself but also against its complexes with Zn^{2+} and potentially with other metal ions. Our data also support further development of CLR01, because CLR01 inhibits the toxicity of Aβ42 both in the absence and in the presence of Zn^{2+}. CLR01 is also an effective inhibitor of tau aggregation and spreading[67,68] making a particularly attractive lead compound for development of AD therapy.

METHODS

All buffers were prepared using deionized water from a Milli-Q water purification system (Millipore) and analytical grade reagents. NaOH, 3-(*N*-morpholino)propanesulfonic acid (MOPS), 1,1,1,3,3,3-hexafluoro-2-propanol (HFIP), and $ZnCl_2$ were purchased from Sigma-Aldrich. For cell culture, Dulbecco's modified Eagle's medium (DMEM) (ThermoFisher Scientific) was supplemented with 10% heat-inactivated horse serum (HS) (ThermoFisher Scientific), 5% fetal bovine serum (FBS, Invitrogen), and 2% penicillin-streptomycin (P/S, ThermoFisher). Synthetic human Aβ42 was from Anaspec. Aβ(39−42) and Aβ(30−40) were either prepared and purified in-house as described previously[69] or obtained from New England Peptides. Aβ(31−42) was obtained from New England Peptides. CLR01 was prepared as described previously[70] and purified as a sodium salt.

Sample Preparation for Biophysical Characterization. Aβ42 was treated with HFIP to remove pre-existing aggregates as described previously.[71] The resulting dry peptide film was dissolved in a 60 mM NaOH solution comprising 10% of the final volume and then diluted to 50% of the final volume using Milli-Q water, either alone or in the presence of Zn^{2+}. Aβ42-Zn^{2+} mixtures were examined in the absence or presence of the CTFs or CLR01. The mixture solutions were sonicated for 1 min using a bath sonicator, and 50% of the final volume 20 mM sodium phosphate buffer (PB), pH 7.4, was added so that the final PB concentration was 10 mM. Aβ42 concentration was confirmed by UV spectroscopy (ε = 1280 M^{-1} cm^{-1}).

Sample Preparation for Cell Culture. Aβ42 was pretreated with HFIP as described previously.[71] The resulting peptide film was dissolved in 60 mM NaOH comprising less than 0.2% of the desired volume in the wells and sonicated for 1 min. Samples then were diluted to a stock concentration of 83 μM using differentiation media (0.5% FBS, 2% P/S in DMEM), and this solution then was added to the wells to yield a final concentration of 5 or 10 μM Aβ42. In our experience, different batches of Aβ42 often have vastly different toxicity. Therefore, we pretest each batch for its toxicity and use it at a concentration that yields 20−50% reduction of cell viability. CTFs and CLR01 solutions were prepared in a similar manner in differentiation media. Each CTF was tested at the following concentrations: 0.5, 1.5, 5, 15, and 50 μM. Thanks to its higher aqueous solubility,[53] Aβ(39−42) also was tested at a maximal concentration of 100 μM. CLR01 was tested at 1, 3, 10, 30, and 100 μM. One or two microliters of a 1 mM $ZnCl_2$ solution was added to each well, as appropriate, to yield a final concentration of 10 or 20 μM Zn^{2+}.

Thioflavin T Fluorescence Assay. ThT fluorescence was recorded as described previously.[30] Fresh, 100 μL samples of 20 μM Aβ42 and 20 μM ThT in 10 mM PB, pH 7.4, were prepared in a 96-well plate in the absence or presence of 40 μM Zn^{2+} and 100 μM of each CTF or 10, 30, or 100 μM CLR01. In control experiments, the CTFs were incubated in the absence or presence of Zn^{2+} at the same concentrations in the absence of Aβ42. The samples were incubated inside BioTek Synergy HT or HTX Multi-Detection Microplate Readers at 37 °C with orbital shaking at 307 rpm, and ThT fluorescence was measured using excitation: 420/50 nm and emission: 485/20 nm every 15 min for the indicated times.

Circular Dichroism Spectroscopy. Secondary structure analysis by CD was performed as described previously[30] with some modifications. Briefly, fresh, 300−450 μL samples of 20 μM Aβ42 were prepared in the absence or presence of 100 μM of each CTF or CLR01 in 10 mM PB, pH 7.4. During preparation, a 1 mM Zn^{2+} solution was added to half of the samples to obtain a final concentration of 40 μM of Zn^{2+}. The samples were incubated at 37 °C with rotational agitation, and CD spectra were recorded at different time points ranging from 0 (immediately after preparation) to 11 d. CD spectra were recorded using a J-810 Jasco spectropolarimeter and analyzed using SM2 software. The data were smoothed using the Savitzky-Golay algorithm[72] set to a convolution width of 25. The spectra were deconvoluted using Bestel software.[73] Each deconvolution curve is an average of two to three experiments.

Electron Microscopy. The same samples used in the CD experiments were also used for EM. The samples were incubated at 37 °C with agitation and aliquots were taken for TEM examination at different time points up to 17 d. Ten microliter aliquots from each solution were deposited on carbon-coated copper grids and stained with 1% uranyl acetate. These samples were analyzed using a JEM1200-EX electron microscope (JEOL) operated at 120 kV. Images were recorded using a wide-angle BioScan 600W 1k × 1k digital camera and saved using digital micrograph acquisition software (Gatan).

Cell Viability Assays. Cell viability assays were conducted as described previously[51] with the following changes: Rat pheochromocytoma (PC-12) cells were cultured in DMEM, containing 10% heat-inactivated HS, 5% FBS, and 1% P/S at 37 °C in an atmosphere of 5% CO_2. Only cells with a passage number between 9 and 15 were

https://dx.doi.org/10.1021/acschemneuro.0c00192
ACS Chem. Neurosci. 2020, 11, 2243−2255

utilized for these experiments to minimize a potential phenotype drift due to a high passage number.[74] Cells were plated at a density of 20 000 per well. Peptide solutions containing 5 or 10 μM Aβ42, 2 mol equiv of $ZnCl_2$ (i.e., 10 or 20 μM, respectively), and increasing concentrations of CTFs or CLR01 were added to the cells. As has been reported previously,[30] to observe the toxicity of Aβ42-Zn^{2+} complexes, fresh samples of each preparation, including Aβ42, Aβ42-Zn^{2+}, or Aβ42-Zn^{2+} in the presence of CTFs or CLR01 were added to the cells every 12 h (i.e., at t = 0, 12, 24, and 36 h). At these time points, 12.5 μL of media were removed from each well, and 12.5 μL of fresh samples were added to each well. At t = 48 h, cell viability was determined using the lactate dehydrogenase release assay and/or the 3-(4,5-dimethylthiazol-2-yl)-2,5-diphenyltetrazolium bromide reduction assay.

■ ASSOCIATED CONTENT

Supporting Information

The Supporting Information is available free of charge at https://pubs.acs.org/doi/10.1021/acschemneuro.0c00192.

Morphological evaluation of Aβ42 incubated in the absence or presence of Zn^{2+} (PDF)

■ AUTHOR INFORMATION

Corresponding Author

Gal Bitan − *Department of Neurology, David Geffen School of Medicine, Brain Research Institute, and Molecular Biology Institute, University of California at Los Angeles, Los Angeles, California 90095, United States;* orcid.org/0000-0001-7046-3754; Phone: 310-206 2082; Email: gbitan@mednet.ucla.edu; Fax: 310-206 1700

Authors

Ashley J. Mason − *Department of Neurology, David Geffen School of Medicine, University of California at Los Angeles, Los Angeles, California 90095, United States*

Ian Hurst − *Department of Neurology, David Geffen School of Medicine, University of California at Los Angeles, Los Angeles, California 90095, United States*

Ravinder Malik − *Department of Neurology, David Geffen School of Medicine, University of California at Los Angeles, Los Angeles, California 90095, United States*

Ibrar Siddique − *Department of Neurology, David Geffen School of Medicine, University of California at Los Angeles, Los Angeles, California 90095, United States*

Inna Solomonov − *Department of Biological Regulation, Weizmann Institute of Science, Rehovot, Israel*

Irit Sagi − *Department of Biological Regulation, Weizmann Institute of Science, Rehovot, Israel*

Frank-Gerrit Klärner − *Institute of Organic Chemistry, University of Duisburg-Essen, Essen 45117, Germany*

Thomas Schrader − *Institute of Organic Chemistry, University of Duisburg-Essen, Essen 45117, Germany;* orcid.org/0000-0002-7003-6362

Complete contact information is available at: https://pubs.acs.org/10.1021/acschemneuro.0c00192

Author Contributions

G.B. designed the research. A.J.M., I.H., R.M., and I.S. performed the research. F.G.K. and T.S. provided unique resources. A.J.M., I.H., and G.B. wrote the manuscript. I. So, I. Sa, F.G.K., and T.S. provided critical reading and discussion of the manuscript.

Author Contributions

#(A.J.M. and I.H.) These authors contributed equally to the work.

Notes

The authors declare no competing financial interest.

■ ACKNOWLEDGMENTS

The work was supported by United States−Israel Binational Science Foundation, Grant No. 2007187 (I.S. and G.B.), NIH/NIA R01AG050721 (G.B.), and the UCLA Mary S. Easton Endowment (G.B.).

■ REFERENCES

(1) Alzheimer, A. (1906) Über einen eigenartigen schweren Erkrankungsprozeβ der Hirnrinde. *Neurologisches Centralblatt 23*, 1129−1136.

(2) Glenner, G. G., and Wong, C. W. (1984) Alzheimer's disease: initial report of the purification and characterization of a novel cerebrovascular amyloid protein. *Biochem. Biophys. Res. Commun. 120* (3), 885−90.

(3) Hardy, J. A., and Higgins, G. A. (1992) Alzheimer's disease: the amyloid cascade hypothesis. *Science 256* (5054), 184−185.

(4) Selkoe, D. J. (1994) Alzheimers disease: A central role for amyloid. *J. Neuropathol. Exp. Neurol. 53* (5), 438−447.

(5) Klein, W. L., Stine, W. B., Jr., and Teplow, D. B. (2004) Small assemblies of unmodified amyloid β-protein are the proximate neurotoxin in Alzheimer's disease. *Neurobiol. Aging 25* (5), 569−580.

(6) Kayed, R., Head, E., Thompson, J. L., McIntire, T. M., Milton, S. C., Cotman, C. W., and Glabe, C. G. (2003) Common structure of soluble amyloid oligomers implies common mechanism of pathogenesis. *Science 300* (5618), 486−489.

(7) Gong, Y., Chang, L., Viola, K. L., Lacor, P. N., Lambert, M. P., Finch, C. E., Krafft, G. A., and Klein, W. L. (2003) Alzheimer's disease-affected brain: presence of oligomeric Aβ ligands (ADDLs) suggests a molecular basis for reversible memory loss. *Proc. Natl. Acad. Sci. U. S. A. 100* (18), 10417−22.

(8) Barghorn, S., Nimmrich, V., Striebinger, A., Krantz, C., Keller, P., Janson, B., Bahr, M., Schmidt, M., Bitner, R. S., Harlan, J., Barlow, E., Ebert, U., and Hillen, H. (2005) Globular amyloid β-peptide oligomer − a homogenous and stable neuropathological protein in Alzheimer's disease. *J. Neurochem. 95* (3), 834−847.

(9) Pitschke, M., Prior, R., Haupt, M., and Riesner, D. (1998) Detection of single amyloid β-protein aggregates in the cerebrospinal fluid of Alzheimer's patients by fluorescence correlation spectroscopy. *Nat. Med. 4* (7), 832−834.

(10) Klein, W. L., Krafft, G. A., and Finch, C. E. (2001) Targeting small Aβ oligomers: the solution to an Alzheimer's disease conundrum? *Trends Neurosci. 24* (4), 219−24.

(11) Lambert, M. P., Barlow, A. K., Chromy, B. A., Edwards, C., Freed, R., Liosatos, M., Morgan, T. E., Rozovsky, I., Trommer, B., Viola, K. L., Wals, P., Zhang, C., Finch, C. E., Krafft, G. A., and Klein, W. L. (1998) Diffusible, nonfibrillar ligands derived from Aβ_{1-42} are potent central nervous system neurotoxins. *Proc. Natl. Acad. Sci. U. S. A. 95* (11), 6448−53.

(12) Hardy, J. (2003) The relationship between amyloid and tau. *J. Mol. Neurosci. 20* (2), 203−6.

(13) Rahimi, F., Li, H., Sinha, S., and Bitan, G. Modulators of Amyloid β-Protein (Aβ) Self-Assembly. In *Developing Therapeutics for Alzheimer's Disease;* Wolfe, M. S., Ed.; Academic Press: Boston, MA, 2016; pp 97−191.

(14) Cuajungco, M. P., Frederickson, C. J., and Bush, A. I. (2005) Amyloid-β metal interaction and metal chelation. *Subcell Biochem 38*, 235−54.

(15) Roberts, B. R., Ryan, T. M., Bush, A. I., Masters, C. L., and Duce, J. A. (2012) The role of metallobiology and amyloid-β peptides in Alzheimer's disease. *J. Neurochem. 120* (1), 149−66.

(16) Wang, P., and Wang, Z. Y. (2017) Metal ions influx is a double edged sword for the pathogenesis of Alzheimer's disease. *Ageing Res. Rev. 35*, 265−290.
(17) Noy, D., Solomonov, I., Sinkevich, O., Arad, T., Kjaer, K., and Sagi, I. (2008) Zinc-amyloid β interactions on a millisecond time-scale stabilize non-fibrillar Alzheimer-related species. *J. Am. Chem. Soc. 130* (4), 1376−83.
(18) Hane, F., and Leonenko, Z. (2014) Effect of metals on kinetic pathways of amyloid-β aggregation. *Biomolecules 4* (1), 101−16.
(19) Faller, P., Hureau, C., and Berthoumieu, O. (2013) Role of metal ions in the self-assembly of the Alzheimer's amyloid-β peptide. *Inorg. Chem. 52* (21), 12193−206.
(20) Warmlander, S., Tiiman, A., Abelein, A., Luo, J., Jarvet, J., Soderberg, K. L., Danielsson, J., and Graslund, A. (2013) Biophysical studies of the amyloid β-peptide: interactions with metal ions and small molecules. *ChemBioChem 14* (14), 1692−704.
(21) Parthasarathy, S., Long, F., Miller, Y., Xiao, Y., McElheny, D., Thurber, K., Ma, B., Nussinov, R., and Ishii, Y. (2011) Molecular-level examination of Cu2+ binding structure for amyloid fibrils of 40-residue Alzheimer's β by solid-state NMR spectroscopy. *J. Am. Chem. Soc. 133* (10), 3390−400.
(22) Miller, Y., Ma, B., and Nussinov, R. (2010) Zinc ions promote Alzheimer Aβ aggregation via population shift of polymorphic states. *Proc. Natl. Acad. Sci. U. S. A. 107* (21), 9490−5.
(23) Lovell, M. A., Robertson, J. D., Teesdale, W. J., Campbell, J. L., and Markesbery, W. R. (1998) Copper, iron and zinc in Alzheimer's disease senile plaques. *J. Neurol. Sci. 158* (1), 47−52.
(24) Tõugu, V., Karafin, A., Zovo, K., Chung, R. S., Howells, C., West, A. K., and Palumaa, P. (2009) Zn(II)- and Cu(II)-induced non-fibrillar aggregates of amyloid-β (1−42) peptide are transformed to amyloid fibrils, both spontaneously and under the influence of metal chelators. *J. Neurochem. 110* (6), 1784−95.
(25) Bishop, G. M., and Robinson, S. R. (2004) The amyloid paradox: amyloid-β-metal complexes can be neurotoxic and neuroprotective. *Brain Pathol. 14* (4), 448−52.
(26) Lovell, M. A., Xie, C., and Markesbery, W. R. (1999) Protection against amyloid β peptide toxicity by zinc. *Brain Res. 823* (1−2), 88−95.
(27) Yoshiike, Y., Tanemura, K., Murayama, O., Akagi, T., Murayama, M., Sato, S., Sun, X., Tanaka, N., and Takashima, A. (2001) New insights on how metals disrupt amyloid β-aggregation and their effects on amyloid-β cytotoxicity. *J. Biol. Chem. 276* (34), 32293−9.
(28) Raman, B., Ban, T., Yamaguchi, K., Sakai, M., Kawai, T., Naiki, H., and Goto, Y. (2005) Metal ion-dependent effects of clioquinol on the fibril growth of an amyloid {β} peptide. *J. Biol. Chem. 280* (16), 16157−62.
(29) Abelein, A., Graslund, A., and Danielsson, J. (2015) Zinc as chaperone-mimicking agent for retardation of amyloid β peptide fibril formation. *Proc. Natl. Acad. Sci. U. S. A. 112* (17), 5407−12.
(30) Solomonov, I., Korkotian, E., Born, B., Feldman, Y., Bitler, A., Rahimi, F., Li, H., Bitan, G., and Sagi, I. (2012) Zn^{2+}−Aβ40 complexes form metastable quasi-spherical oligomers that are cytotoxic to cultured hippocampal neurons. *J. Biol. Chem. 287* (24), 20555−64.
(31) Watt, N. T., Whitehouse, I. J., and Hooper, N. M. (2010) The role of zinc in Alzheimer's disease. *Int. J. Alzheimers Dis 2011*, 971021.
(32) Bush, A. I. (2003) The metallobiology of Alzheimer's disease. *Trends Neurosci. 26* (4), 207−14.
(33) Frederickson, C. J., Klitenick, M. A., Manton, W. I., and Kirkpatrick, J. B. (1983) Cytoarchitectonic distribution of zinc in the hippocampus of man and the rat. *Brain Res. 273* (2), 335−9.
(34) Li, Y., Hough, C. J., Suh, S. W., Sarvey, J. M., and Frederickson, C. J. (2001) Rapid translocation of Zn(2+) from presynaptic terminals into postsynaptic hippocampal neurons after physiological stimulation. *J. Neurophysiol. 86* (5), 2597−604.
(35) Ali, F. E., Barnham, K. J., Barrow, C. J., and Separovic, F. (2004) Metal catalyzed oxidation of tyrosine residues by different oxidation systems of copper/hydrogen peroxide. *J. Inorg. Biochem. 98* (1), 173−84.
(36) Lacor, P. N., Buniel, M. C., Furlow, P. W., Clemente, A. S., Velasco, P. T., Wood, M., Viola, K. L., and Klein, W. L. (2007) Aβ oligomer-induced aberrations in synapse composition, shape, and density provide a molecular basis for loss of connectivity in Alzheimer's disease. *J. Neurosci. 27* (4), 796−807.
(37) Townsend, M., Shankar, G. M., Mehta, T., Walsh, D. M., and Selkoe, D. J. (2006) Effects of secreted oligomers of amyloid β-protein on hippocampal synaptic plasticity: a potent role for trimers. *J. Physiol. 572*, 477−492.
(38) Maynard, C. J., Bush, A. I., Masters, C. L., Cappai, R., and Li, Q. X. (2005) Metals and amyloid-β in Alzheimer's disease. *Int. J. Exp. Pathol. 86* (3), 147−59.
(39) Adlard, P. A., Parncutt, J., Lal, V., James, S., Hare, D., Doble, P., Finkelstein, D. I., and Bush, A. I. (2015) Metal chaperones prevent zinc-mediated cognitive decline. *Neurobiol. Dis. 81*, 196−202.
(40) Deshpande, A., Kawai, H., Metherate, R., Glabe, C. G., and Busciglio, J. (2009) A role for synaptic zinc in activity-dependent Aβ oligomer formation and accumulation at excitatory synapses. *J. Neurosci. 29* (13), 4004−15.
(41) Faux, N. G., Ritchie, C. W., Gunn, A., Rembach, A., Tsatsanis, A., Bedo, J., Harrison, J., Lannfelt, L., Blennow, K., Zetterberg, H., Ingelsson, M., Masters, C. L., Tanzi, R. E., Cummings, J. L., Herd, C. M., and Bush, A. I. (2010) PBT2 rapidly improves cognition in Alzheimer's Disease: additional phase II analyses. *J. Alzheimer's Dis. 20* (2), 509−16.
(42) Huang, L., Lu, C., Sun, Y., Mao, F., Luo, Z., Su, T., Jiang, H., Shan, W., and Li, X. (2012) Multitarget-directed benzylideneindanone derivatives: anti-β-amyloid (Aβ) aggregation, antioxidant, metal chelation, and monoamine oxidase B (MAO-B) inhibition properties against Alzheimer's disease. *J. Med. Chem. 55* (19), 8483−92.
(43) Su, T., Zhang, T., Xie, S., Yan, J., Wu, Y., Li, X., Huang, L., and Luo, H. B. (2016) Discovery of novel PDE9 inhibitors capable of inhibiting Aβ aggregation as potential candidates for the treatment of Alzheimer's disease. *Sci. Rep. 6*, 21826.
(44) Lee, S., Zheng, X., Krishnamoorthy, J., Savelieff, M. G., Park, H. M., Brender, J. R., Kim, J. H., Derrick, J. S., Kochi, A., Lee, H. J., Kim, C., Ramamoorthy, A., Bowers, M. T., and Lim, M. H. (2014) Rational design of a structural framework with potential use to develop chemical reagents that target and modulate multiple facets of Alzheimer's disease. *J. Am. Chem. Soc. 136* (1), 299−310.
(45) Sharma, A. K., Pavlova, S. T., Kim, J., Finkelstein, D., Hawco, N. J., Rath, N. P., Kim, J., and Mirica, L. M. (2012) Bifunctional compounds for controlling metal-mediated aggregation of the aβ42 peptide. *J. Am. Chem. Soc. 134* (15), 6625−36.
(46) Jokar, S., Khazaei, S., Behnammanesh, H., Shamloo, A., Erfani, M., Beiki, D., and Bavi, O. (2019) Recent advances in the design and applications of amyloid-β peptide aggregation inhibitors for Alzheimer's disease therapy. *Biophys. Rev. 11*, 901−925.
(47) Knez, D., Coquelle, N., Pislar, A., Zakelj, S., Jukic, M., Sova, M., Mravljak, J., Nachon, F., Brazzolotto, X., Kos, J., Colletier, J. P., and Gobec, S. (2018) Multi-target-directed ligands for treating Alzheimer's disease: Butyrylcholinesterase inhibitors displaying antioxidant and neuroprotective activities. *Eur. J. Med. Chem. 156*, 598−617.
(48) Wichur, T., Wieckowska, A., Wieckowski, K., Godyn, J., Jonczyk, J., Valdivieso, A. D. R., Panek, D., Pasieka, A., Sabate, R., Knez, D., Gobec, S., and Malawska, B. (2020) 1-Benzylpyrrolidine-3-amine-based BuChE inhibitors with anti-aggregating, antioxidant and metal-chelating properties as multifunctional agents against Alzheimer's disease. *Eur. J. Med. Chem. 187*, 111916.
(49) Xu, P., Zhang, M., Sheng, R., and Ma, Y. (2017) Synthesis and biological evaluation of deferiprone-resveratrol hybrids as antioxidants, Aβ1−42 aggregation inhibitors and metal-chelating agents for Alzheimer's disease. *Eur. J. Med. Chem. 127*, 174−186.
(50) Feng, B. Y., Shelat, A., Doman, T. N., Guy, R. K., and Shoichet, B. K. (2005) High-throughput assays for promiscuous inhibitors. *Nat. Chem. Biol. 1* (3), 146−8.

https://dx.doi.org/10.1021/acschemneuro.0c00192
ACS Chem. Neurosci. 2020, 11, 2243−2255

(51) Fradinger, E. A., Monien, B. H., Urbanc, B., Lomakin, A., Tan, M., Li, H., Spring, S. M., Condron, M. M., Cruz, L., Xie, C. W., Benedek, G. B., and Bitan, G. (2008) C-terminal peptides coassemble into Aβ42 oligomers and protect neurons against Aβ42-induced neurotoxicity. *Proc. Natl. Acad. Sci. U. S. A. 105* (37), 14175−80.
(52) Li, H., Du, Z., Lopes, D. H., Fradinger, E. A., Wang, C., and Bitan, G. (2011) *C*-Terminal tetrapeptides inhibit Aβ42-induced neurotoxicity primarily through specific interaction at the *N*-Terminus of Aβ42. *J. Med. Chem. 54* (24), 8451−60.
(53) Li, H., Monien, B. H., Fradinger, E. A., Urbanc, B., and Bitan, G. (2010) Biophysical characterization of Aβ42 *C*-terminal fragments: inhibitors of Aβ42 neurotoxicity. *Biochemistry 49* (6), 1259−67.
(54) Li, H., Monien, B. H., Lomakin, A., Zemel, R., Fradinger, E. A., Tan, M., Spring, S. M., Urbanc, B., Xie, C. W., Benedek, G. B., and Bitan, G. (2010) Mechanistic investigation of the inhibition of Aβ42 assembly and neurotoxicity by Aβ42 *C*-terminal fragments. *Biochemistry 49* (30), 6358−64.
(55) Li, H., Rahimi, F., and Bitan, G. (2016) Modulation of Amyloid β-Protein (Aβ) Assembly by Homologous C-Terminal Fragments as a Strategy for Inhibiting Aβ Toxicity. *ACS Chem. Neurosci. 7* (7), 845−56.
(56) Good, N. E., Winget, G. D., Winter, W., Connolly, T. N., Izawa, S., and Singh, R. M. (1966) Hydrogen ion buffers for biological research. *Biochemistry 5* (2), 467−77.
(57) Sinha, S., Lopes, D. H., Du, Z., Pang, E. S., Shanmugam, A., Lomakin, A., Talbiersky, P., Tennstaedt, A., McDaniel, K., Bakshi, R., Kuo, P. Y., Ehrmann, M., Benedek, G. B., Loo, J. A., Klärner, F. G., Schrader, T., Wang, C., and Bitan, G. (2011) Lysine-specific molecular tweezers are broad-spectrum inhibitors of assembly and toxicity of amyloid proteins. *J. Am. Chem. Soc. 133* (42), 16958−69.
(58) Gessel, M. M., Wu, C., Li, H., Bitan, G., Shea, J. E., and Bowers, M. T. (2012) Aβ(39−42) modulates Aβ oligomerization but not fibril formation. *Biochemistry 51* (1), 108−17.
(59) Kirkitadze, M. D., Condron, M. M., and Teplow, D. B. (2001) Identification and characterization of key kinetic intermediates in amyloid β-protein fibrillogenesis. *J. Mol. Biol. 312* (5), 1103−19.
(60) Attar, A., and Bitan, G. (2014) Disrupting self-assembly and toxicity of amyloidogenic protein oligomers by " molecular tweezers" − from the test tube to animal models. *Curr. Pharm. Des. 20* (15), 2469−83.
(61) Schrader, T., Bitan, G., and Klärner, F. G. (2016) Molecular tweezers for lysine and arginine - powerful inhibitors of pathologic protein aggregation. *Chem. Commun. (Cambridge, U. K.) 52* (76), 11318−34.
(62) Hadrovic, I., Rebmann, P., Klärner, F. G., Bitan, G., and Schrader, T. (2019) Molecular Lysine Tweezers Counteract Aberrant Protein Aggregation. *Front Chem. 7*, 657.
(63) Wilch, C., Talbiersky, P., Berchner-Pfannschmidt, U., Schaller, T., Kirsch, M., Klärner, F. G., and Schrader, T. (2017) Molecular Tweezers Inhibit PARP-1 by a New Mechanism. *Eur. J. Org. Chem. 2017* (16), 2223−2229.
(64) Herzog, G., Shmueli, M. D., Levy, L., Engel, L., Gazit, E., Klärner, F. G., Schrader, T., Bitan, G., and Segal, D. (2015) The Lys-Specific Molecular Tweezer, CLR01, Modulates Aggregation of the Mutant p53 DNA Binding Domain and Inhibits Its Toxicity. *Biochemistry 54* (24), 3729−38.
(65) Li, H., Zemel, R., Lopes, D. H., Monien, B. H., and Bitan, G. (2012) A two-step strategy for structure-activity relationship studies of *N*-methylated Aβ42 C-terminal fragments as Aβ42 toxicity inhibitors. *ChemMedChem 7* (3), 515−22.
(66) Sinha, S., Du, Z., Maiti, P., Klärner, F. G., Schrader, T., Wang, C., and Bitan, G. (2012) Comparison of three amyloid assembly inhibitors: the sugar *scyllo*-inositol, the polyphenol epigallocatechin gallate, and the molecular tweezer CLR01. *ACS Chem. Neurosci. 3* (6), 451−8.
(67) Attar, A., Ripoli, C., Riccardi, E., Maiti, P., Li Puma, D. D., Liu, T., Hayes, J., Jones, M. R., Lichti-Kaiser, K., Yang, F., Gale, G. D., Tseng, C. H., Tan, M., Xie, C. W., Straudinger, J. L., Klärner, F. G., Schrader, T., Frautschy, S. A., Grassi, C., and Bitan, G. (2012) Protection of primary neurons and mouse brain from Alzheimer's pathology by molecular tweezers. *Brain 135*, 3735−48.
(68) Despres, C., Di, J., Cantrelle, F. X., Li, Z., Huvent, I., Chambraud, B., Zhao, J., Chen, J., Chen, S., Lippens, G., Zhang, F., Linhardt, R., Wang, C., Klarner, F. G., Schrader, T., Landrieu, I., Bitan, G., and Smet-Nocca, C. (2019) Major Differences between the Self-Assembly and Seeding Behavior of Heparin-Induced and in Vitro Phosphorylated Tau and Their Modulation by Potential Inhibitors. *ACS Chem. Biol. 14* (6), 1363−1379.
(69) Condron, M. M., Monien, B. H., and Bitan, G. (2008) Synthesis and purification of highly hydrophobic peptides derived from the C-terminus of amyloid β-protein. *Open Biotechnol. J. 2* (1), 87−93.
(70) Talbiersky, P., Bastkowski, F., Klärner, F. G., and Schrader, T. (2008) Molecular clip and tweezer introduce new mechanisms of enzyme inhibition. *J. Am. Chem. Soc. 130* (30), 9824−9828.
(71) Rahimi, F., Maiti, P., and Bitan, G. (2009) Photo-induced cross-linking of unmodified proteins (PICUP) applied to amyloidogenic peptides. *J. Vis. Exp.* No. 23, No. e1071.
(72) Savitzky, A., and Golay, M. J. E. (1964) Smoothing and Differentiation of Data by Simplified Least Squares Procedures. *Anal. Chem. 36* (8), 1627−1639.
(73) Micsonai, A., Wien, F., Kernya, L., Lee, Y. H., Goto, Y., Refregiers, M., and Kardos, J. (2015) Accurate secondary structure prediction and fold recognition for circular dichroism spectroscopy. *Proc. Natl. Acad. Sci. U. S. A. 112* (24), E3095−103.
(74) Kinarivala, N., Shah, K., Abbruscato, T. J., and Trippier, P. C. (2017) Passage Variation of PC12 Cells Results in Inconsistent Susceptibility to Externally Induced Apoptosis. *ACS Chem. Neurosci. 8* (1), 82−88.

https://dx.doi.org/10.1021/acschemneuro.0c00192
ACS Chem. Neurosci. 2020, 11, 2243−2255